Title

Cytosolic bacterial pathogens activate TLR pathways in tumors that synergistically enhance STING agonist cancer therapies

Authors

Danielson, Meggie
Nicolai, Chris J
Vo, Thaomy T
et al.

Publication Date

2024-11-01

DOI

10.1016/j.isci.2024.111385

iScience

Article

Cytosolic bacterial pathogens activate TLR pathways in tumors that synergistically enhance STING agonist cancer therapies

Graphical abstract

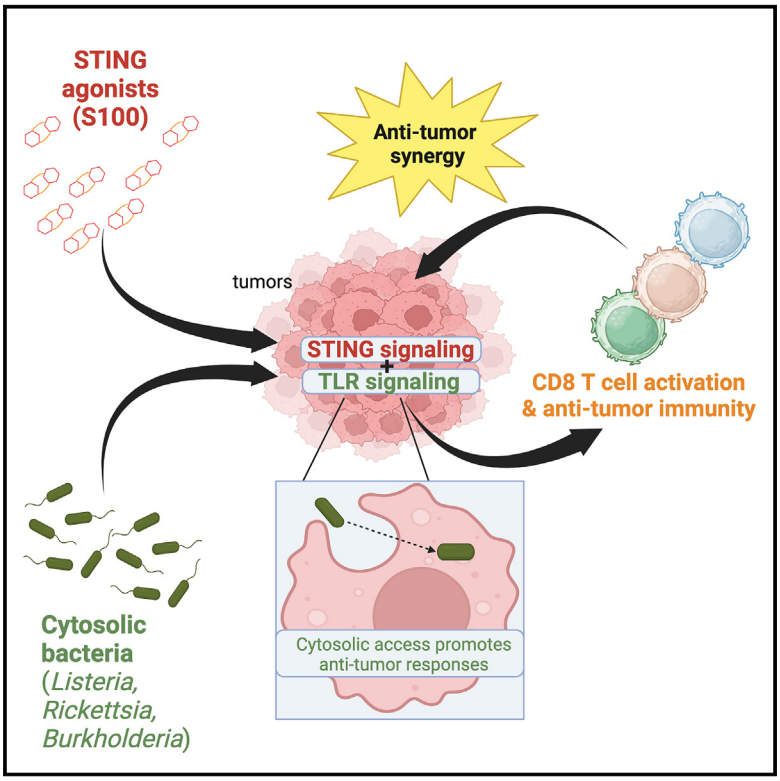

Highlights

- Intratumoral delivery of cytosolic bacterial pathogens elicits anti-tumor responses
- Anti-tumor responses are independent cGAS/STING but require TLR signaling
- Combining pathogens with STING agonists elicits profound anti-tumor synergy
- Establishes framework to improve microbial cancer therapies

Authors

Meggie Danielson, Christopher J. Nicolai, Thaomy T. Vo, Natalie K. Wolf, Thomas P. Burke

Correspondence

tpburke@uci.edu

In brief

Health sciences; Molecular biology; Molecular mechanism of gene regulation

Danielson et al., 2024, iScience 27, 111385
December 20, 2024
https://doi.org/10.1016/j.isci.2024.111385

CellPress

iScience

CellPress
OPEN ACCESS

Article

Cytosolic bacterial pathogens activate TLR pathways in tumors that synergistically enhance STING agonist cancer therapies

Meggie Danielson,[1] Christopher J. Nicolai,[2] Thaomy T. Vo,[1] Natalie K. Wolf,[2] and Thomas P. Burke[1,3,*]
[1]Microbiology and Molecular Genetics, University of California, Irvine, Irvine, CA 92617, USA
[2]Molecular and Cell Biology, University of California, Berkeley, Berkeley, CA 94720, USA
[3]Lead contact
*Correspondence: tpburke@uci.edu
https://doi.org/10.1016/j.isci.2024.111385

SUMMARY

Intracellular bacterial pathogens are distinctive tools for fighting cancer, as they can proliferate in tumors and deliver therapeutic payloads to the eukaryotic cytosol. Cytosol-dwelling bacteria have undergone extensive preclinical and clinical testing, yet the mechanisms of activating innate immunity in tumors are unclear. We report that phylogenetically distinct cytosolic pathogens, including *Listeria*, *Rickettsia*, and *Burkholderia* species, elicited anti-tumor responses in poorly immunogenic melanoma and lymphoma in mice. Although the bacteria required cytosolic access, anti-tumor responses were largely independent of the cytosolic sensors cyclic GMP-AMP synthase (cGAS) and stimulator of interferon genes (STING), but instead required Toll-like receptor (TLR) signaling. Combining pathogens with STING agonists elicited profound, synergistic anti-tumor effects with complete responses in >80% of mice. Small molecule TLR agonists also synergistically enhanced STING agonists. The responses required RAG2 but not interferons, and cured mice developed immunity to cancer rechallenge requiring $CD8^+$ T cells. These studies provide a framework for enhancing microbial and small molecule innate agonists for cancer, via co-activating STING and TLRs.

INTRODUCTION

Bacteria that invade the eukaryotic cytosol are distinctive tools for treating cancer, as they can be engineered to deliver cancer antigens to MHC-I, which elicits potent anti-tumor $CD8^+$ T cell responses.[1] Many bacteria that are eliminated in other organs can proliferate in tumors, as this tissue is immunosuppressed and hypoxic.[1] Bacterial vaccine platforms have undergone extensive preclinical testing and human clinical trials. However, the contributions made by innate immunity to the anti-cancer response elicited by microbes are unclear. Activating innate immune receptors with small molecules in the tumor microenvironment (TME) elicits potent anti-tumor effects and has resulted in FDA-approval of anti-cancer drugs,[2] and therefore activation of these pathways by microbial vaccine platforms may contribute to their anti-cancer effects. Understanding the molecular mechanisms by which cytosolic bacterial pathogens elicit anti-tumor responses will enhance our ability to design novel microbial and small molecule-based therapies for cancer immunotherapy.

Pattern recognition receptors (PRRs) detect pathogen-associated molecular patterns (PAMPs) and elicit pro-inflammatory cytokine responses that protect against infection. Toll-like receptors (TLRs) are membrane bound PRRs that detect extracellular or endosomal microbial ligands. TLRs recruit cytosolic adaptors including MyD88 and TRIF to activate transcription factors including NF-κB, resulting in the secretion of pro-inflammatory cytokines such as tumor necrosis factor α (TNF-α).[3] In contrast to membrane-bound TLRs, the protein cyclic GMP-AMP synthase (cGAS) binds mislocalized DNA in the cytosol as a signature of infection.[4] cGAS then synthesizes the cyclic dinucleotide (CDN) 2′3′ cyclic GMP-AMP (cGAMP), which binds to and activates stimulator of interferon genes (STING). STING activates Tank-binding kinase 1 (TBK1) and interferon responsive factor 3 (IRF3), causing a robust inflammatory response hallmarked by production of type I interferon (IFN-I), TNF-α, and chemokines.[5]

Listeria monocytogenes (*Lm*), *Rickettsia parkeri* (*Rp*), and *Burkholderia thailandensis* (*Bt*) are three distantly related pathogens that share a similar intracellular life cycle of replicating directly in the cytosol of mammalian cells. However, despite residing in the same cytosolic compartment, *Lm*, *Bt*, and *Rp* have distinct relationships with PRRs. *Lm* is a gram-positive foodborne pathogen that activates STING via the secretion of the CDN cyclic-di-AMP, and *Lm* also activates TLR2 and Myd88 *in vivo*.[6,7] In contrast, *Rp* is a gram-negative tick-borne pathogen whose bacteriolysis can activate cGAS, but this activation is masked by inflammasome-mediated cell death.[8] Mice lacking the lipopolysaccharide receptor TLR4 have increased susceptibility to rickettsial infection, suggesting that *Rp* also activates TLRs *in vivo*.[9] *Bt* is a gram-negative soil-dwelling microbe that is avirulent in humans, as it is strongly restricted by inflammasomes and is detected by TLRs.[10] Its interactions with cGAS/STING are uncharacterized.

As cytosolic pathogens, these microbes have the capacity to deliver antigens to MHC-I, and *Lm* has undergone human clinical trials as a cancer vaccine platform,[11–14] yet the underlying mechanisms by which *Lm*, *Rp*, and *Bt* activate innate immunity in tumors are unknown.

Bacterial pathogens hold the potential to robustly activate innate immunity for cancer immunotherapy. For example, *Mycobacterium bovis* bacillus Calmette-Guerin (BCG) is approved for treating non-muscle invasive bladder cancer. Activating innate immunity with small molecule TLR agonists has also been successful in the clinic, for example imiquimod targets TLR7 and is FDA-approved for basal cell carcinoma. Intratumoral delivery of small molecule STING agonists potently inhibits tumor growth in preclinical models.[5,15–18] STING agonists activate $CD8^+$ T and NK cells and elicit long-lasting memory against cancer rechallenge.[15,19–21] However, human clinical trials using intratumoral delivery of STING agonists were not efficacious,[22,23] demonstrating the need for new approaches that enhance STING agonist therapies for cancer immunotherapy.

Here, we investigated how cytosolic bacterial pathogens activate innate immunity in tumors. We report that *Lm*, *Rp*, and *Bt* inhibited the growth of multiple, poorly immunogenic tumors in mice with no observable toxicity. We were surprised to find that the pathogens required cytosolic access for inducing anti-tumor effects, yet the anti-tumor activity was independent of cGAS/STING and instead required TLR signaling. Live bacteria were more efficacious than killed bacteria or small molecule TLR agonists, suggesting that there are advantages to using live microbes and that their replication likely stimulates multiple host pathways. When combined with STING agonists, cytosolic pathogens elicited striking, synergistic anti-tumor effects and immunity to cancer cell rechallenge. Small molecule TLR agonists recapitulated synergy when combined with STING agonists. The combination therapy elicited long-lasting immunity against cancer cell rechallenge that required $CD8^+$ T cells. Together, this study reveals underlying mechanisms by which microbes elicit anti-tumor responses and suggests that co-activation of STING and TLR pathways with microbes or small molecules elicits synergistic anti-tumor responses. This work provides critical insights into how microbes and small molecule can be designed to robustly activate innate immunity for cancer immunotherapy.

RESULTS

Intratumoral delivery of cytosolic bacterial pathogens elicits dose-dependent anti-tumor responses in multiple non-immunogenic murine tumor models

It was unknown whether intratumoral delivery of cytosolic bacterial pathogens elicited anti-tumor responses and if intratumoral delivery caused toxicity *in vivo*. To limit any potential toxicity, we used *Lm* Δ*actA*Δ*inlB*, which underwent phase 1 and 2 clinical trials and is tolerated in humans at doses of $>10^9$ bacteria.[11–14,24] This strain is also >1,000-fold attenuated for virulence in mice.[24,25] We used WT *Rp*, which does not elicit disease in WT mice[26] and *Rp* mutants lacking the actin-based motility factor Sca2, which is required for cell-to-cell spread and promotes dissemination *in vivo*.[27] We used a *Bt* strain lacking the motility factors BimA and MotA2. C57Bl/6j mice were implanted subcutaneously with 10^6 B16-F10 cells, which are syngeneic poorly immunogenic melanoma cells. Approximately 7 days later when tumor sizes measured ~6 mm (width) x 6 mm (length) x 2.5 mm (depth), tumors were intratumorally injected with 10^7 Δ*actA*Δ*inlB* *Lm*, Δ*bimA*Δ*motA2* *Bt*, *sca2*:Tn *Rp*, or WT *Rp* (mutants referred to as *Lm*, *Rp*, and *Bt* unless otherwise indicated). Each bacterial pathogen elicited a significant decrease in tumor volume as compared to vehicle PBS and promoted significantly longer survival (Figure 1A). The anti-tumor effects were largely similar between the different pathogens. Male and female mice were included in each group, and no significant differences were observed between sexes (Figure S1). To determine if pathogens elicited anti-tumor effects in a different cancer indication, we measured tumor volume after intratumoral delivery of *Rp* to RMA lymphoma xenografts, which are poorly immunogenic syngeneic models of lymphoma.[21] Pathogen delivery resulted in a significant delay in tumor growth and resulted in complete responses in ~25% of mice (Figure 1B). Among all the bacterial strains tested, no mice were euthanized due to apparent bacteremia. These data demonstrate that intratumoral delivery of phylogenetically distinct cytosolic bacterial pathogens elicits anti-cancer effects with limited/no bacterial-related toxicity.

It remained unclear if the anti-tumor effects were dose dependent and we therefore measured tumor volume upon delivery of varying doses of *Lm*, *Bt*, and *Rp*. Delivery of $5x10^7$, 10^7, and 10^6 *Lm* all elicited anti-tumor responses, while 10^7 and $5x10^7$ elicited significantly longer survival than 10^6, and no differences were observed between the two highest doses (Figure 1C). No differences were observed between the doses of *Bt* (Figure 1D). Delivering higher doses of *Rp* significantly improved the anti-tumor response (Figure 1E). These data demonstrate that the anti-tumoral effects of these pathogens are somewhat dose-dependent and that 10^7 bacteria mostly maximizes the anti-tumor response without eliciting toxicity. We therefore delivered 10^7 bacteria for the remaining experiments.

Cytosolic access promotes the bacterial anti-tumor response

It remained unknown whether the anti-tumor effects required live bacteria to access the cytosol. We asked whether non-pathogenic *Escherichia coli* or heat-killed *Rp* elicited robust anti-tumor responses in B16-F10 tumors. Intratumoral delivery of heat-killed *Rp* or live non-pathogenic *E. coli* did not significantly delay tumor growth (Figure 2A) and had a minor but significant effect on survival (Figure 2A). To determine if the anti-tumor effects required access to the cytosol, we measured tumor growth after delivery of an *Lm* strain mutated for the hemolysin listeriolysin-O (LLO; encoded by the gene *hly*). *hly* mutants are unable to perforate the vacuole and are confined to membrane-bound intracellular compartments *in vitro*. We found that the *Lm* Δ*hly* strain did not elicit robust anti-tumor responses or improve overall survival (Figure 2B). These data demonstrate that cytosolic access is necessary for eliciting a robust anti-tumor response.

The microbe-mediated antitumor effects are independent of cGAS/STING but require TLR signaling

It was unclear if the anti-tumor effects of *Lm*, *Bt*, and *Rp* required innate immune signaling. As cytosolic access was necessary for

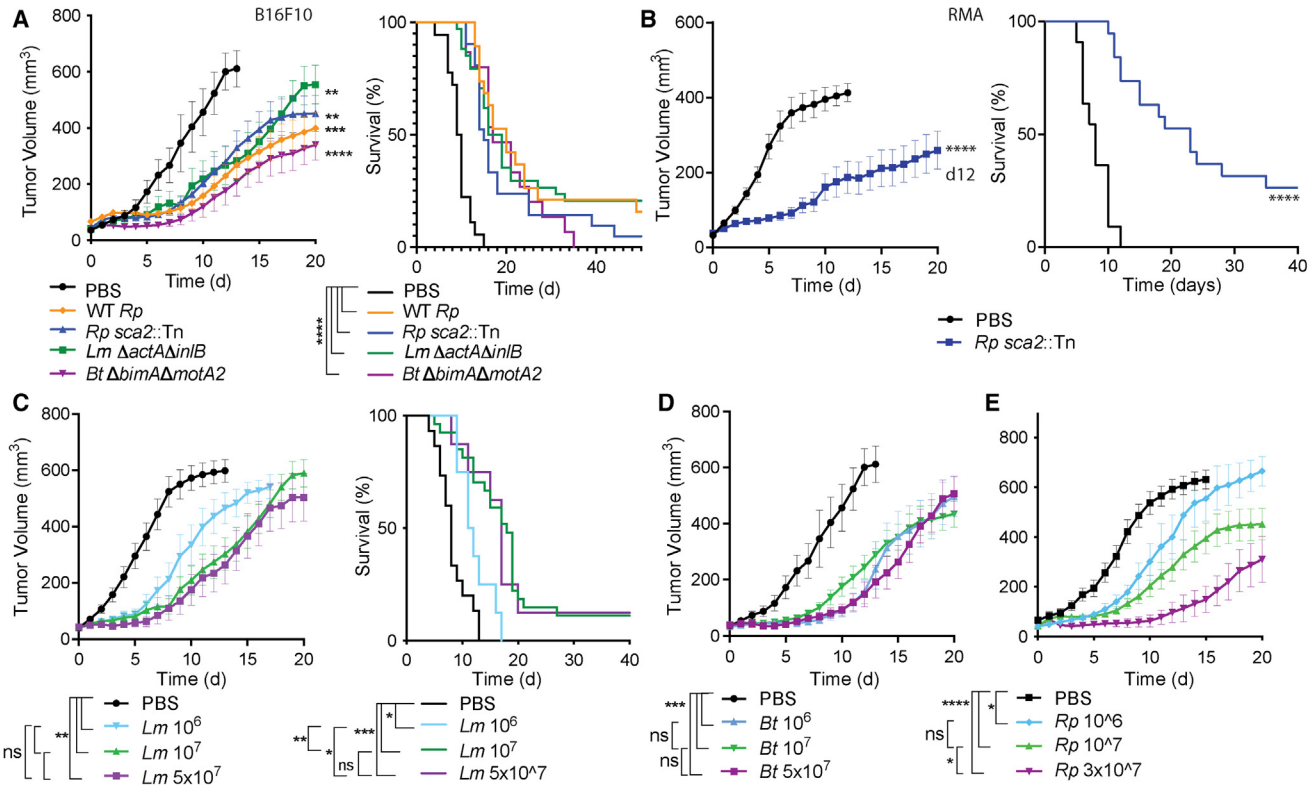

Figure 1. Intratumoral delivery of cytosolic bacterial pathogens elicits dose-dependent anti-tumor responses in multiple non-immunogenic murine tumor models

(A) Tumor volume (left) and overall survival (right) of mice bearing B16-F10 tumors after intratumoral delivery of 10^7 the indicated strains at d = 0.

(B) RMA-bearing C57bl/6j mice were intratumorally injected with PBS or 10^7 *Rp sca2*:Tn.

(C–E) Tumor volume over time of B16-F10-bearing mice treated with (C) *Lm ΔactAΔinlB*; (D) *Bt ΔbimAΔmotA2*; or (E) *Rp sca2*:Tn. Statistics for tumor growth used two-way ANOVA from days 0–20, or if animals were euthanized prior to day 20 the comparisons were made from day 0 up until the final day (day 13 in panels C, D, day 15 in panel E). Statistics for survival used log rank (Mantel-Cox) tests. *$p < 0.05$; **$p < 0.01$; ***$p < 0.001$; ****$p < 0.0001$, ns = not significant. Data for each graph are the combination of at least two separate experiments with a total of at least 8 mice per experimental group. Tumor volume data are means +/- SEM. Tumors were injected on the day that they measured approximately 6 × 6 × 2.5 mm in each direction. Tumor volumes are shown as ellipsoids using the formula: $V = (\pi/6)ABC$.

the anti-tumor effects, we hypothesized that the anti-tumor effects may be mediated through cGAS and STING. We therefore measured B16-F10 tumor volume in *Cgas*$^{-/-}$ and *Sting*$^{gt/gt}$ mice after pathogen delivery. Contrary to our hypothesis, we observed that tumor volume after *Lm* delivery was similar between WT mice and *Cgas*$^{-/-}$ mice (Figure 3A) and between WT mice and *Sting*$^{gt/gt}$ mice (Figure 3B). Similarly, the anti-tumor effects of *Rp* were similar between WT and *Cgas*$^{-/-}$ mice (Figure 3C) and *Sting*$^{gt/gt}$ mice (Figure 3D). STING did not promote survival after *Lm* or *Rp* therapy (Figure 3E). This suggested that the role for STING in eliciting the anti-tumor effects to these pathogens was minor. It remained a possibility that cGAS signaling in the tumor cells themselves was promoting the anti-tumor response. To determine if cGAS signaling in the tumor cells contributed to the anti-tumor effects, we delivered pathogens to *Cgas*$^{-/-}$ tumors implanted in WT and *Cgas*$^{-/-}$ mice. The microbes elicited a similar anti-tumor effect when *Cgas*$^{-/-}$ tumor cells were implanted into either WT or *Cgas*$^{-/-}$ mice (Figure 3F), demonstrating that the antitumor response is largely independent of cGAS. Together, these data suggest that cGAS and STING are not critical for the anti-tumor effects mediated by cytosolic bacterial pathogens.

We next investigated whether other innate immune pathways were required for the microbial anti-tumor effects. Since *Lm*, *Rp*, and *Bt* can activate TLRs in other contexts,[6,7,9,10] and because the anti-tumor effects *M. bovis* BCG bacteria require TLR signaling,[28] we hypothesized that TLR activation contributed to the anti-tumor effects. We measured the anti-tumor responses of pathogens in *Myd88*$^{-/-}$*Trif*$^{-/-}$ mice and observed diminished tumor control after treatment with *Rp* (Figure 3G) or *Lm* (Figure 3H), suggesting that TLR signaling is an important driver of the response. To further explore the role for TLR signaling, we hypothesized that co-administration of bacterial pathogens with small molecule TLR agonists would not dramatically enhance the anti-tumor effects. Indeed, there was no enhanced effect of combining *Lm* with the TLR2 agonist PAM3CSK4, which actually significantly decreased the anti-tumor effects of *Lm* (Figure 3I). We hypothesized that if the effects were mainly TLR driven, bacterial mutants deficient for lipoprotein synthesis would elicit reduced anti-tumor responses. *Lm* lipoprotein synthesis requires the phosphatidylglycerol-prolipoprotein diacylglyceryl transferase (LGT) and *lgt* mutants fail to activate TLR2 *in vivo*.[29] We compared the anti-tumor effects of *ΔactAΔinlB*

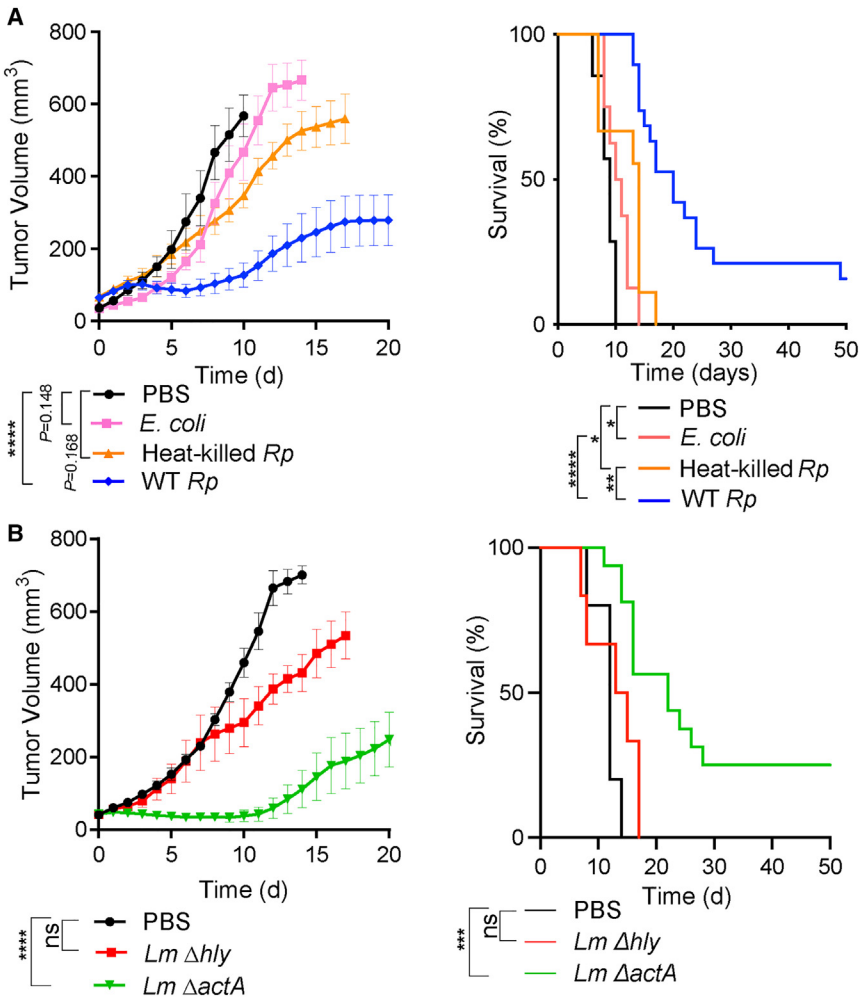

Figure 2. Cytosolic access of bacteria promotes the anti-tumor response

(A and B) Mice bearing B16-F10 tumors were intratumorally injected with 10^7 of the indicated strains at day 0 and tumor volume and survival were monitored over time. Tumor volume data are means +/- SEM. Statistics for tumor growth used ANOVA at day 10 (A) or day 13 (B) as compared to vehicle PBS; statistics for survival used log rank (Mantel-Cox) tests; *p < 0.05; **p < 0.01; ***p < 0.001; ****p < 0.0001; ns = not significant.

Lm versus *ΔactAΔinlBΔlgt* and observed that strains lacking LGT had a significantly reduced anti-tumor effect (Figure 3J). Taken together, these data demonstrate that, although the bacteria require cytosolic access, TLR signaling but not cGAS or STING signaling is a critical driver of the anti-tumor response to cytosolic pathogens.

Rag2 is required while IFNs are largely dispensable for the microbe-mediated anti-tumor effects

We next sought to better define the role for inflammatory cytokines to the anti-tumor response elicited by cytosolic bacteria. IFN-I plays complex roles for a variety of cancer therapies, however, it is not critical for the anti-tumor response elicited by BCG.[30] We observed that mice lacking the receptor for IFN-I (IFNAR) had slightly weaker but insignificant (p = 0.07) anti-tumor responses to *Lm* as compared to WT mice (Figure 4A), suggesting that IFN-I only minorly contributes to the anti-tumor activities of *Lm*. We also investigated the role for IFN-γ, another pro-inflammatory cytokine that can elicit pro- or anti-tumor responses in different contexts.[31] We observed that mice lacking the receptor for IFN-γ (IFNGR) also had slightly weaker but insignificant (p = 0.13) anti-tumor responses as compared to WT mice (Figure 4B). Survival of *Ifnar*$^{-/-}$ or *Ifngr*$^{-/-}$ mice treated with *Lm* was not significantly different from WT mice (Figure 4C). As a control, we also measured tumor volume in response to dithio-containing cyclic di-AMP (aka S100, ADU-S100, MIW815, ML RR-S2 CDA, or 2′3′-RR CDA).[15] In alignment with previous reports[20] we found that it required IFNAR (Figure 4D). Together, these findings suggest that signaling through individual interferon receptors is largely dispensable to the anti-tumor responses elicited by cytosolic bacteria.

We next sought to determine the role for immune cell types in the microbe-mediated anti-tumor response. We delivered *Lm* to tumor-bearing *Rag2*$^{-/-}$ mice, which lack mature T and B cells. *Rag2*$^{-/-}$ mice had similar tumor growth as WT mice from 0 to 12 days (Figure 4E). However, all *Rag2*$^{-/-}$ mice had to be euthanized by day 12 due to tumor volume size, and WT mice survived significantly longer (Figure 4F), suggesting that T cells play critical roles in the anti-tumor effects of cytosolic bacteria. Together, these experiments suggest that individual cytokines may only play minor roles in the anti-tumor effects elicited by microbial cancer therapies, whereas T cells are critical.

The STING agonist S100 synergistically enhances the anti-tumor effects of cytosolic bacterial pathogens

The observation that bacterial pathogens elicit TLR-dependent anti-tumor responses led us to hypothesize that their effects would be enhanced by STING agonists. We therefore evaluated the anti-tumor effects of *Lm*, *Bt*, and *Rp* in combination with the eukaryotic cGAS product 2′3′-cGAMP (referred to here as cGAMP) or S100. S100 binds STING with higher affinity than cGAMP and underwent preclinical and clinical development.[15,20,22,23] To maximize the potential for observing differences between therapies, each tumor was treated with only one dose of each therapy at d = 0. Additionally, we used combinations of male and female mice that were over 18 weeks old, as we had observed that <14-week-old mice respond significantly stronger to STING agonists than 18+ week old mice (Figure S2). We hypothesized that this higher threshold model would allow us

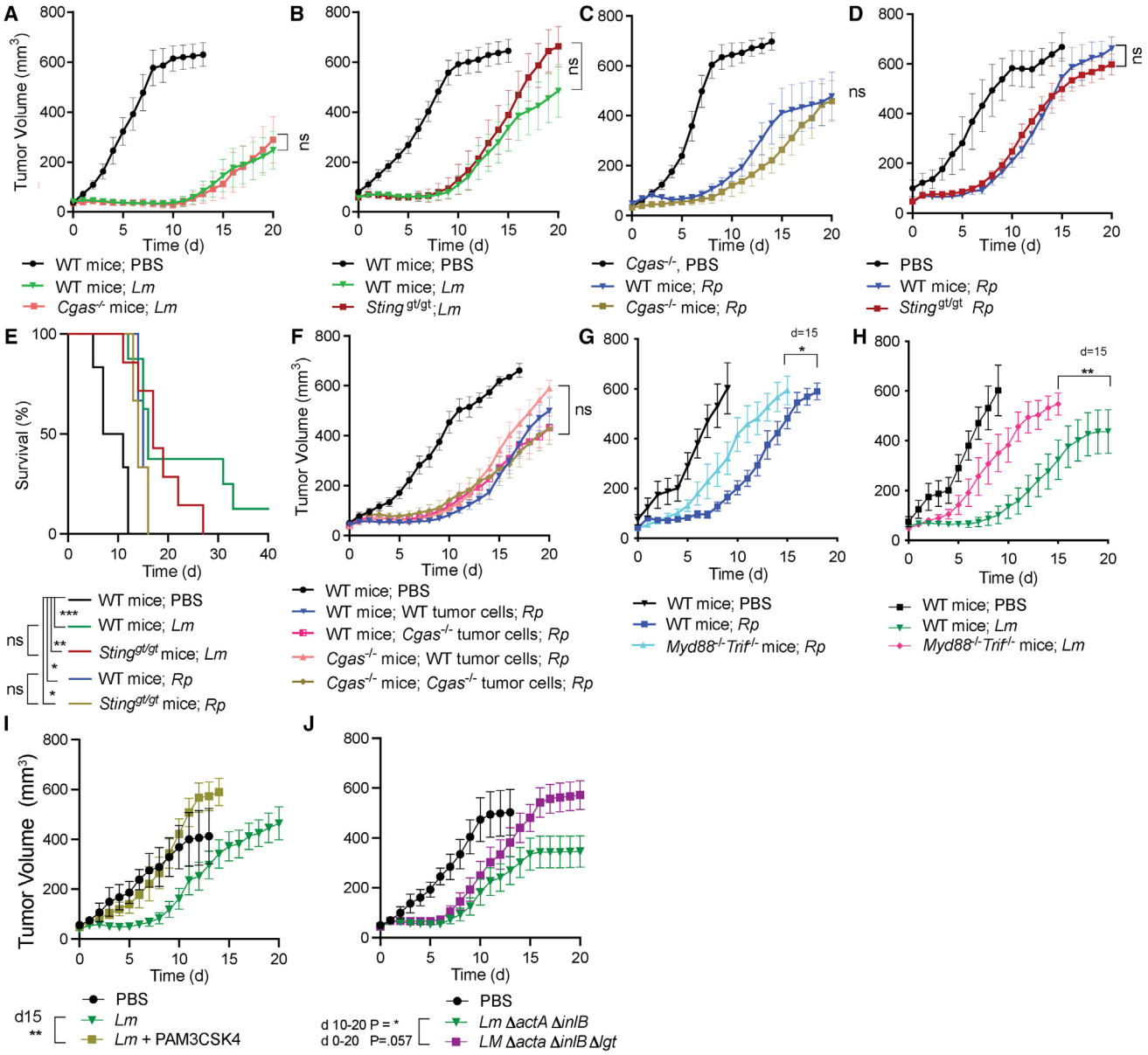

Figure 3. The microbe-mediated anti-tumor effects are largely independent of cGAS/STING but require TLR signaling

(A–J) Tumor-bearing mice were intratumorally administered with 10^7 of bacteria and tumor volume and survival were monitored over time. For (A–E) and (G–J), B16-F10 tumor cells were used, and for (F) B16-BL6 cells were used. For (A–J) *Lm* was Δ*actA*Δ*inlB* and *Rp* was *sca2*:Tn. For (I) 10 μg of TLR2 agonist PAM3CSK4 (Invivogen) was used. Tumor volume data are means +/- SEM. Statistics for tumor growth used two-way ANOVA at day 20 unless otherwise indicated; statistics for survival used log rank (Mantel-Cox) tests. *$p < 0.05$; **$p < 0.01$; ***$p < 0.001$; ****$p < 0.0001$; ns = not significant.

to better observe differences between S100 and S100+pathogen combination therapy. Upon combining with S100, we observed striking and synergistic anti-tumor effects with *Lm* (Figure 5A), *Rp*, (Figure 5B) and *Bt* (Figure 5C). In contrast, cGAMP did not significantly enhance the anti-tumor effects of *Lm*, *Rp*, or *Bt* when compared to cGAMP alone (Figures 5D–5F). Combination therapy with S100 dramatically improved overall survival with *Lm*, *Rp*, and *Bt* (Figures 5G–5I). In the case of *Lm*, combination therapy with S100 elicited complete responses in 9 of 11 mice (82%), while monotherapy with either S100 or *Lm* alone only led to complete clearance in only ~25% of tumor-bearing mice (Figure 5G). Together, these data demonstrate that the anti-tumor effects of bacteria can be dramatically enhanced upon co-administration with STING agonists.

Pathogens + STING agonists do not synergistically increase IFN-I production *in vitro*, and IFNs are not critical for the anti-tumor response *in vivo*

As bacterial pathogens may potentially exacerbate or inhibit IFN-I or IFN-γ production, we sought to determine how IFN-I

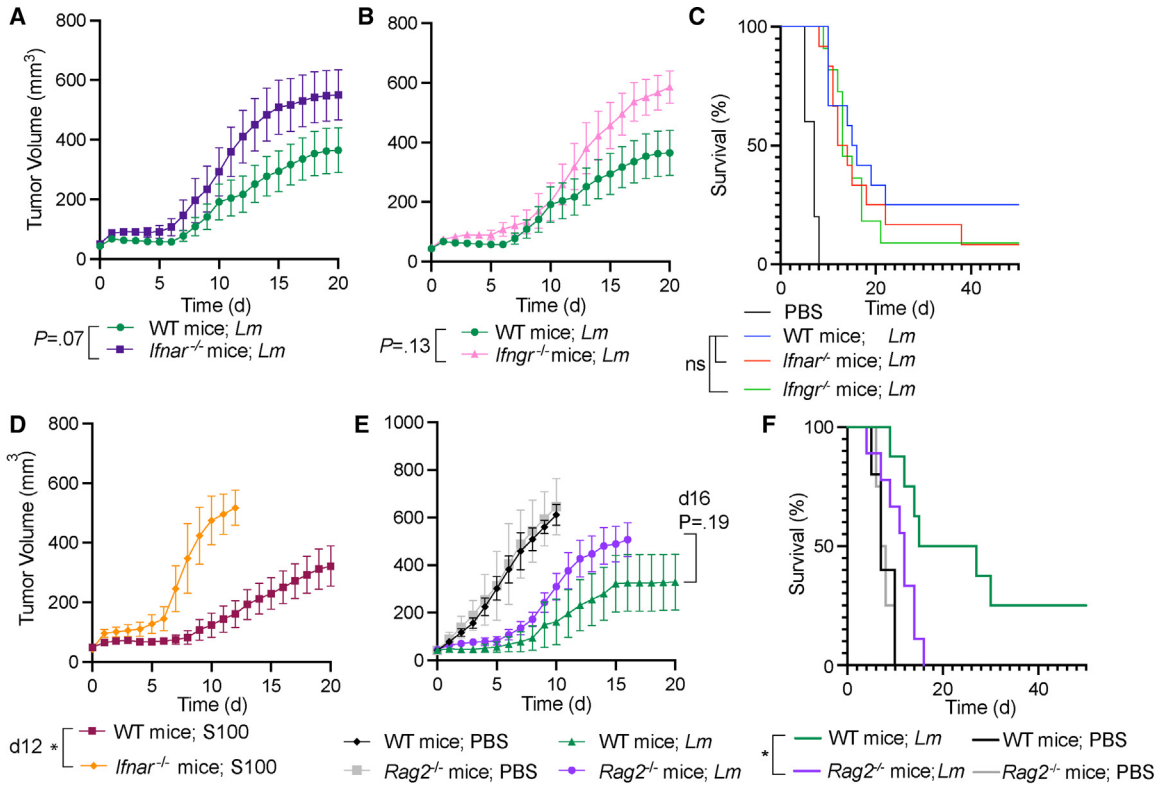

Figure 4. RAG2 is required for the microbe-mediated anti-tumor effects, while IFNAR or IFNGR are largely dispensable

(A–F) B16-F10 tumor bearing mice were intratumorally administered with 10^7 of the indicated bacterial strains and tumor volume and survival were monitored over time. 50 μg of S100 was used, which was combined with the bacteria immediately prior to injection. Tumor volume data are means +/- SEM. Statistics for tumor growth used two-way ANOVA at day 20 unless indicated at an earlier day. Statistics for survival used log rank (Mantel-Cox) tests. Data combined from a minimum of two experiments in which each group had a total minimum of 8 mice. *$p < 0.05$.

production was affected upon treatment of infected murine bone marrow-derived macrophages (BMDMs) with STING agonists. S100 still caused robust IFN-I production when added to cells infected with *Lm*, *Bt*, or *Rp*. In each case, IFN-I production was similar between infected and uninfected cells (Figure 6A). Together this led us to conclude that STING agonists elicit robust cytokine production in cells infected with cytosolic bacterial pathogens. *In vivo*, we had found that IFN-I signaling was required for the anti-tumor effects of S100 (Figure 4C) but not *Lm* (Figure 4A), yet the role for IFNs in STING+TLR combination therapy was unclear. We therefore examined whether pathogen + CDN combination therapy required IFN-I or IFN-γ signaling. We observed that upon treatment of *Ifnar*$^{-/-}$ and *Ifngr*$^{-/-}$ mice, the combination *Lm* + S100 therapy elicited an anti-tumor response that was similar to that elicited in WT mice (Figure 6B). This suggests that the anti-tumor cytokine response is likely multifaceted and only partially requires individual cytokines such as IFN-I or IFN-γ.

Small molecule TLR agonists synergize with STING agonists

We next asked whether small molecule TLR agonists synergized with STING agonists. As we observed that the production of *Lm* lipoproteins was required for the anti-tumor response (Figure 3K), we hypothesized that the lipopeptide PAM3CSK4 would enhance the anti-tumor effects of S100. We observed that S100 anti-tumor activity was dramatically enhanced by the addition of PAM3CSK4 (Figure 7A), as was mouse survival (Figure 7B). Notably, PAM3CSK4 had no anti-tumor effects on its own, in alignment with previous observations,[32] suggesting that the bacterial pathogens activate stronger anti-tumor responses than small molecule TLR2 agonists. Together, these data align with our findings that cytosolic bacteria mostly elicit TLR-dependent anti-tumor responses and suggest a strategy to robustly activate innate immunity for cancer immunotherapy with small molecules, via co-activation STING and TLRs.

Bacterial therapy increases immunity to tumor cell rechallenge

It remained unknown whether mice that received therapy and cleared the initial tumor had a long-lived adaptive immune response against cancer. Previous studies on STING agonist monotherapies found that optimal doses of STING agonists (50 μg) elicited maximum T cell responses, whereas higher doses (500 μg) caused T cell apoptosis.[20,33] Therefore, it was unclear whether STING+TLR combination therapy would elicit effective long-lasting immunity in comparison to STING agonist monotherapy. We examined if mice that rejected tumors after

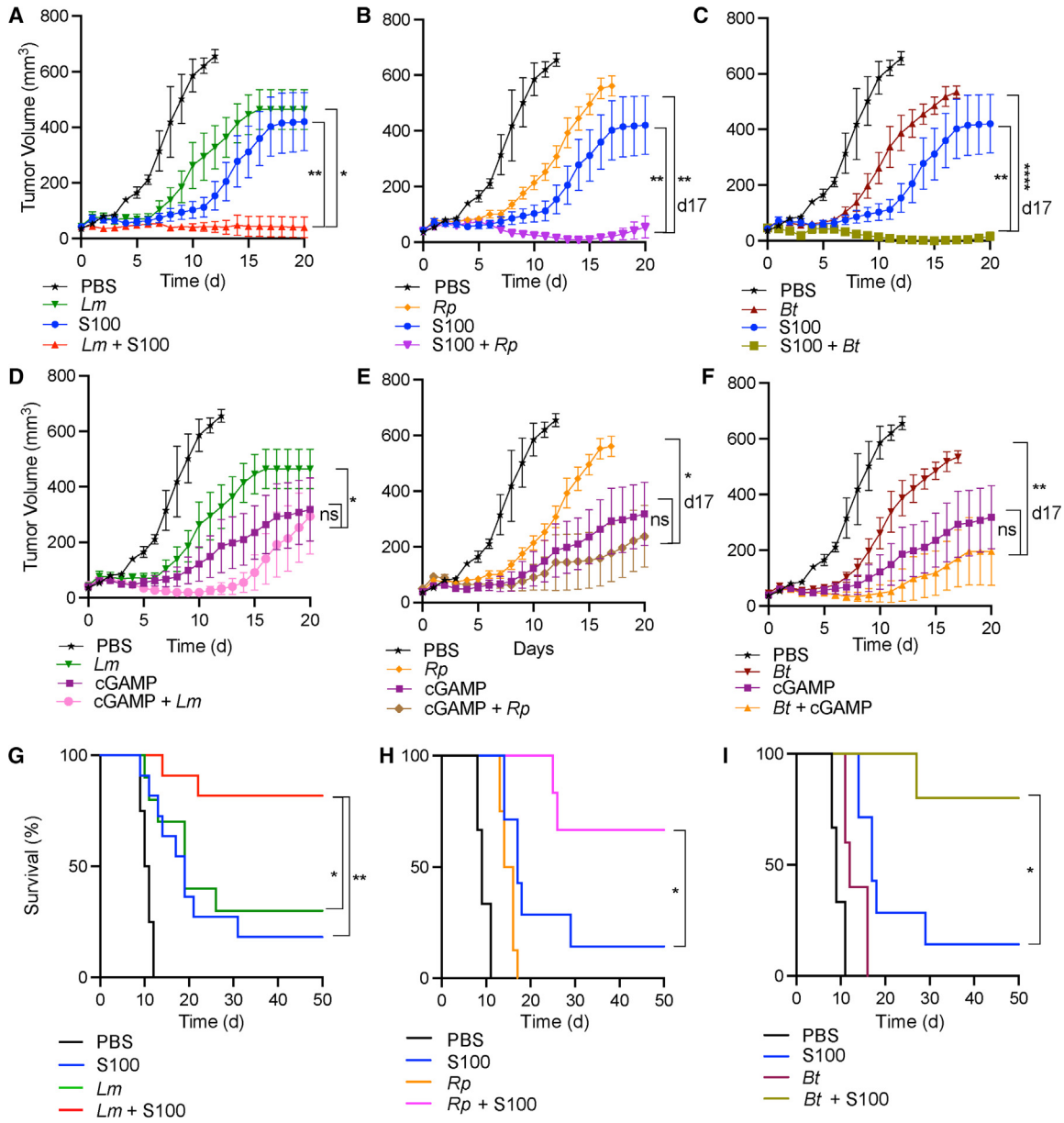

Figure 5. The anti-tumor effects of bacterial pathogens synergize with the STING agonist S100

(A–I) B16-F10 tumor volume and survival was measured over time after intratumoral delivery with the indicated bacterial species and innate immune agonists. cGAMP (Invivogen) and S100 (Chemietek) were used at 50 μg/mouse and were combined with the bacteria immediately prior to injection. The strains used were *Lm* Δ*actA*Δ*inlB* (*Lm*), *Bt* Δ*bimA*Δ*motA2* (*Bt*), or *Rp sca2*:Tn (*Rp*). A single injection was performed for all therapies at d = 0. Data are combined from a minimum of two experiments in which each group had a total minimum of 6 mice. Tumor volume data are means +/- SEM. Statistics for tumor growth used ANOVA at day 20 unless otherwise indicated; statistics for survival used log rank (Mantel-Cox) tests. *$p < 0.05$; **$p < 0.01$; ***$p < 0.001$; ****$p < 0.0001$; ns = not significant.

treatment developed tumors after re-administration of the same tumor cell line >40 days later. We found that mice that cleared initial B16-F10 tumors by the bacteria, bacteria + CDN combination therapy, or S100 + PAM3CSK4 combination therapy had increased immunity against rechallenge as compared to naive mice (Figure 8A). Interestingly, mice cleared of tumors from bacteria alone had enhanced survival as compared to CDN or CDN + bacteria combination therapies. Cured mice that were treated with CDNs alone versus combination therapies had similar survival (Figure 8A). Importantly, this suggests that the addition of TLR agonists enhances the anti-tumor effects of STING agonists without causing a detriment to long-lasting immunity.

To determine if this protective immunity was T cell dependent, we depleted $CD8^+$ T cells in mice that cleared the initial tumor and then rechallenged them with 10^6 B16-F10 tumor cells in the opposite flank. Mice depleted for CD8 T cells demonstrated a decreased ability to reject the tumor cell rechallenge (Figure 8B). These findings demonstrate that intratumoral delivery

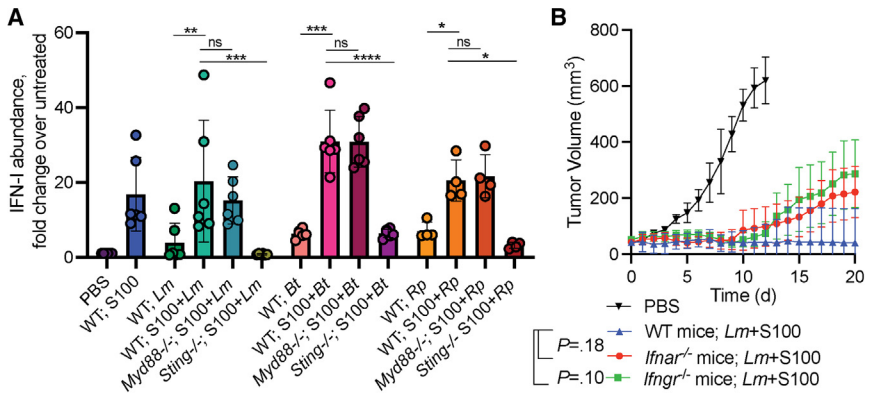

Figure 6. IFN-I induction by STING agonists is maintained in infected cells *in vitro*, and IFNs are not critical for the anti-tumor response *in vivo*

(A) BMDMs were infected with *Lm* Δ*actA*Δ*inlB* (*Lm*), *Bt* Δ*bimA*Δ*motA2* (*Bt*), or *Rp sca2*:Tn (*Rp*) at an MOI of 1. 200 ng of S100 was added immediately after infection and supernatants were collected at 7 hpi. Supernatants were used to stimulate an IFN-I-responsive cell line (ISRE-luciferase) and relative light units (RLUs) were measured 4 h later. Data are combined from ≥3 independent experiments. Data were analyzed using a one-way ANOVA with Tukey's multiple comparisons test.

(B) B16-F10 tumor volume and survival was measured over time after intratumoral delivery with 10^7 *Lm* Δ*actA*Δ*inlB* and 50 μg S100. A single injection was performed for all therapies at d = 0. Data are combined from three independent experiments. Tumor volume data are means +/- SEM. Statistics for tumor growth used two-way ANOVA at day 20; *$p < 0.05$; **$p < 0.01$; ***$p < 0.001$; ****$p < 0.0001$; ns = not significant.

of cytosolic bacterial pathogens and combinational therapy of pathogens with STING agonists elicits long-lasting protective immune responses against cancer that require $CD8^+$ T cells.

DISCUSSION

Bacteria have been used to treat cancer since the 1890s and they are the first examples of immunotherapy.[1] Cytosolic bacterial pathogens are particularly important microbial tools, as they can be engineered to deliver tumor antigens and other cancer drugs to the eukaryotic cytosol. Yet, the mechanisms by which cytosolic bacterial pathogens elicit anti-tumor responses and activate innate immunity in tumors have remained unknown. Here, we find that phylogenetically distinct species of cytosol-dwelling bacterial pathogens elicit anti-tumor responses in multiple tumor models in mice. The anti-tumor responses require access to the cytosol, but are largely independent of cGAS/STING, and instead require TLR signaling. Combining cytosolic pathogens with STING agonists elicits a striking and synergistic anti-tumor effect that clears injected tumors with a high frequency and elicits a long-lasting $CD8^+$ T cell response against cancer. This strategy is highly effective even with a single injection into established, poorly immunogenic B16-F10 melanomas in both male and female mice that were >18 weeks old. We propose that co-activation of STING and TLRs is a robust strategy for designing new generations of microbial and small molecule-based innate immune agonist therapies.

Bacteria are being tested clinically as vehicles to deliver STING agonists, including a non-pathogenic *E. coli* Nissle strain engineered to express cyclic di-AMP in the tumor.[34] Intratumoral injection of this strain to B16-F10 tumor-bearing mice induces IFN-I production and reduces tumor growth.[35] This study also found that *E. coli* activate TLRs *in vitro*. In a phase I clinical trial (NCT04167137), this cyclic di-AMP-expressing *E. coli* strain was delivered intratumorally as monotherapy or in combination with atezolizumab and demonstrated safety and cytokine production.[34] Based on our findings, we speculate that this approach may be activating TLR and STING pathways, although the magnitude of these effects when compared to a cocktail of STING agonists and *E. coli* is unknown. As we found that bacteria combined with S100 elicit synergistic anti-tumor responses while cGAMP does not, we predict that the efficacy of microbial therapies would be improved if they are able to secrete agonists with enhanced binding affinity for STING. Another novel bacterial-based immunotherapy is an attenuated *Salmonella* Typhimurium strain (STACT) that carries an inhibitor of TREX-1, the exonuclease that prevents activation of STING by degrading cytosolic DNA. Pre-clinical work found that intravenous delivery caused tumor colonization, tumor regression, and immunity to rechallenge.[5] Such microbial-based cancer therapies are advantageous as they can be administrated systemically and thus can target tumors throughout the body. However, in these studies the role for co-activation of STING and TLRs has not been defined, and based on our work we hypothesize that a lynchpin for their efficacy is robust activation of STING and TLRs.

Our results suggest that live cytosolic bacteria pathogens elicit superior anti-tumor responses as compared to heat-killed bacteria, non-pathogenic bacteria, vacuolar-confined bacteria, and small molecule TLR2 agonists. We were surprised to observe that the anti-tumor effects require cytosolic access yet require TLRs but not STING. The explanations for how the pathogens trigger TLR-dependent anti-tumor responses and why this requires cytosolic access remain unclear. We speculate that the live bacteria more robustly activate a combination of many PRRs, cell death pathways, and other stress responses that dead bacteria do not. Future studies into which TLRs are required and in what cell types, as well as other host cell death and stress response pathways that are activated in tumors will help elucidate these mechanisms.

This study adds key insights into a growing body of literature demonstrating that combinations of innate immune agonists elicit synergistic anti-tumor responses.[36–45] Previous investigations on the mechanisms of synergy revealed enhanced cytokine secretion, namely IL-12, IFN-I, IFN-γ, and TNF-α.[38,43–45] Cytokines including interferons play multifaceted roles in cancer, in which acute therapeutic activation of STING requires IFN-I signaling for a proper anti-tumor response.[20,46] IFN-I promotes the ability of dendritic cells to cross-present antigen and activate

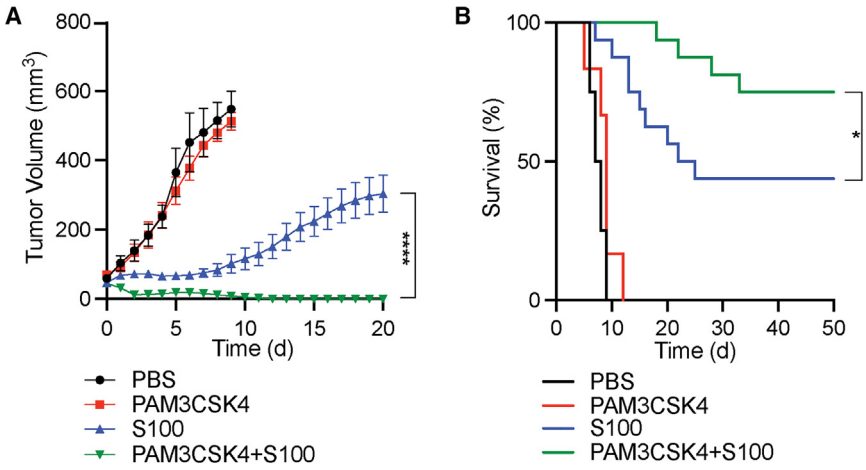

Figure 7. Small molecule STING+TLR agonist combinations elicit synergistic anti-tumor effects

(A and B) B16-F10 tumor volume and survival was measured over time. 10 μg of PAM3CSK4 and 50 μg S100 were used per mouse and were injected into palpable tumors. Agonists were combined immediately prior to injection on day 0. Data are combined from two experiments in which each group had a total minimum of 10 mice. Tumor volume data are means +/- SEM. Statistics for tumor growth used two-way ANOVA at day 20; statistics for survival used log rank (Mantel-Cox) tests. *$p < 0.05$; ****$p < 0.0001$; ns = not significant.

T cells, and CD8a dendritic cells are required to spontaneously prime tumor-specific $CD8^+$ T cells. IFN-I is induced by the TLR7 agonist imiquimod, however, IFN-I does not appear critical for the anti-tumor response elicited by BCG.[30] It was unclear whether these cytokines are necessary for the synergy observed upon STING+TLR agonist combination therapy. Our results with *Ifnar*$^{-/-}$ and *Ifngr*$^{-/-}$ mice reveal that combination therapy can overcome a deficiency in these cytokines, whereas in contrast, STING agonist monotherapy requires IFN-I. This emphasizes the importance of depletion and neutralization studies *in vivo* alongside measuring cytokine and cell type abundance. Many of these previous studies also have relied on cGAMP instead of a drug with higher affinity to STING such as S100. We find that S100 elicits much stronger anti-tumor responses when combined with pathogens than cGAMP, thus emphasizing the need for optimizing both the STING and TLR agonists to maximize the effects of combination therapy.

Spontaneous T cell development against tumors have been shown to improve patients' overall prognosis, and STING agonists elicit long-lasting T cell responses in preclinical models.[15,20,47] In alignment with this, we find that *Rag2*$^{-/-}$ mice have decreased antitumor responses, and CD8 T cell depletion eliminates immunity against tumor rechallenge. One challenge with STING+TLR combination therapy is balancing an anti-tumor response with excessive inflammation can result in inhibitory, apoptotic effects for infiltrating T cells.[20,33] Previous work with STING agonists demonstrated that 50 μg of intratumoral delivery of S100 elicits a strong initial anti-tumor response and also a long-lasting memory response, while higher doses can cause T cell apoptosis to the detriment of the T cell response.[20] We find that the combinatorial effects of pathogens with STING agonists are highly potent in reducing tumor size, and the cured mice have long-lasting protection that is similar to S100 therapy alone. Thus, enhancing STING agonists with TLR agonist combinations does not detrimentally affect the long-lasting T cell response. Future preclinical studies that closely measure the T cell response to STING+TLR agonist therapy are warranted to determine the optimal drug dosage combinations for eliciting robust anti-tumor responses paired with strong memory responses.

We focused on intratumoral delivery as a methodology that allowed for finely discriminating between the efficacy of microbial, STING, and TLR agonist therapies. However, the intratumoral delivery route is likely not as ideal for treating metastatic cancer

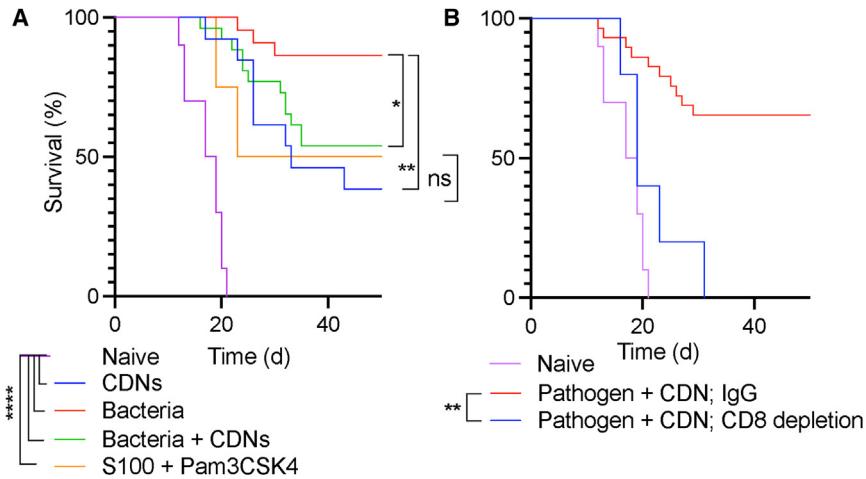

Figure 8. Bacterial cancer therapies elicit immunity to tumor cell rechallenge

(A and B) Survival of mice after rechallenge with B16-F10 tumors. 10^6 B16-F10 cells were implanted subcutaneously into mice which had previously cleared initial tumors after intratumoral delivery of the indicated therapies. Rechallenges were performed a minimum of 40 days after the primary therapy was delivered. For depletions, antibodies were delivered to tumor bearing mice at days −2, −1, and 0 days prior to tumor rechallenge. Data are combined from a minimum of two experiments in which each group had a total minimum of 8 mice. *$p < 0.05$; **$p < 0.01$; ***$p < 0.001$; ****$p < 0.0001$; ns = not significant.

as systemic therapy, which can target multiple inaccessible tumors simultaneously. Thus, developing STING+TLR combination therapies for systemic delivery is a critical future direction for the field. One challenge toward developing systemic therapies with innate immune agonists, however, is that STING and TLRs are widely expressed on many resident tissue cell types, including endothelial cells, macrophages, and monocytes. This hurdle will need to be overcome by specifically targeting tumors, perhaps through tumor-targeting bacteria or small molecules that are activated preferentially in tumors. Targeting both STING and TLRs with such systemic tumor-activated therapies will enhance anti-tumor responses while maintaining T cell responses and is a critical milestone for new generations of innate immune agonists.

RESOURCE AVAILABILITY

Lead contact

Further information and requests for resources and reagents should be directed and will be fulfilled by Dr. Thomas P. Burke (tpburke@uci.edu).

Materials availability

This study did not generate new unique reagents.

Data and code availability

Any additional information required to reanalyze the data reported in this paper is available from the lead contact upon request.

Data

All standardized data have been deposited in the Dryad repository and are publicly available as of the date of publication. Accession numbers are listed in the key resources table.

Code

This paper does not report original code.

Limitations of the study

Limitations of this study include demonstrating synergistic cytokine responses in human cells when infected with pathogens and treated with STING agonists, cytokine profiling *in vivo*, discovering comprehensively which cytokines and cell types are required for the anti-tumor response, and discovering why cytosolic access is necessary for TLR signaling.

ACKNOWLEDGMENTS

T.P.B. was supported in part by ACS Seed Grant 129801-IRG-16-187-13-IRG from the American Cancer Society. C.J.N. was supported by NIH fellowship F31CA228381. N.K.W. was supported by the NSF Predoctoral Fellowship DGE 1752814 and QB3 Frontiers in Medical Research Predoctoral Fellowship.

AUTHOR CONTRIBUTIONS

M.D. and T.P.B. designed, performed, and analyzed experiments. N.W., T.T.V., and C.J.N. contributed to performing experiments. T.P.B. wrote the original draft of this manuscript. Critical reading and edits were provided M.D., N.W., C.J.N., and T.T.V. Supervision was provided by T.P.B.

DECLARATION OF INTERESTS

C.J.N. is employed by Umoja Biopharma. N.W. is employed by Novartis Biomedical Research.

STAR★METHODS

Detailed methods are provided in the online version of this paper and include the following:

- KEY RESOURCES TABLE
- EXPERIMENTAL MODEL AND STUDY PARTICIPANT DETAILS
  - Animal maintenance
  - Mouse genotyping
  - Bacterial strains
  - Preparation of bacteria
  - Deriving bone marrow macrophages
- METHOD DETAILS
  - Tumor xenografts and intratumoral deliveries
  - Infections *in vitro*
  - *In vitro* assays
- QUANTIFICATION AND STATISTICAL ANALYSIS

SUPPLEMENTAL INFORMATION

Supplemental information can be found online at https://doi.org/10.1016/j.isci.2024.111385.

Received: May 20, 2024
Revised: June 4, 2024
Accepted: November 11, 2024
Published: November 13, 2024

REFERENCES

1. Forbes, N.S. (2010). Engineering the perfect (bacterial) cancer therapy. Nat. Rev. Cancer *10*, 785–794.
2. Corrales, L., McWhirter, S.M., Dubensky, T.W., and Gajewski, T.F. (2016). The host STING pathway at the interface of cancer and immunity. J. Clin. Invest. *126*, 2404–2411.
3. Kawasaki, T., and Kawai, T. (2014). Toll-Like Receptor Signaling Pathways. Front. Immunol. *5*, 461.
4. Sun, L., Wu, J., Du, F., Chen, X., and Chen, Z.J. (2013). Cyclic GMP-AMP synthase is a cytosolic DNA sensor that activates the type I interferon pathway. Science *339*, 786–791.
5. Amouzegar, A., Chelvanambi, M., Filderman, J.N., Storkus, W.J., and Luke, J.J. (2021). Sting agonists as cancer therapeutics. Cancers *13*, 2695.
6. Torres, D., Barrier, M., Bihl, F., Quesniaux, V.J.F., Maillet, I., Akira, S., Ryffel, B., and Erard, F. (2004). Toll-Like Receptor 2 Is Required for Optimal Control of Listeria monocytogenes Infection. Infect. Immun. *72*, 2131–2139.
7. Nguyen, B.N., Chávez-Arroyo, A., Cheng, M.I., Krasilnikov, M., Louie, A., and Portnoy, D.A. (2020). TLR2 and endosomal TLR-mediated secretion of IL-10 and immune suppression in response to phagosome-confined listeria monocytogenes. PLoS Pathog. *16*, e1008622.
8. Burke, T.P., Engström, P., Chavez, R.A., Fonbuena, J.A., Vance, R.E., and Welch, M.D. (2020). Inflammasome-mediated antagonism of type I interferon enhances Rickettsia pathogenesis. Nat. Microbiol. *5*, 688–696.
9. Jordan, J.M., Woods, M.E., Olano, J., and Walker, D.H. (2008). The absence of toll-like receptor 4 signaling in C3H/HeJ mice predisposes them to overwhelming rickettsial infection and decreased protective Th1 responses. Infect. Immun. *76*, 3717–3724.
10. Aachoui, Y., Leaf, I.A., Hagar, J.A., Fontana, M.F., Campos, C.G., Zak, D.E., Tan, M.H., Cotter, P.A., Vance, R.E., Aderem, A., and Miao, E.A. (2013). Caspase-11 protects against bacteria that escape the vacuole. Science *339*, 975–978.
11. Le, D.T., Brockstedt, D.G., Nir-Paz, R., Hampl, J., Mathur, S., Nemunaitis, J., Sterman, D.H., Hassan, R., Lutz, E., Moyer, B., et al. (2012). A live-attenuated listeria vaccine (ANZ-100) and a live-attenuated listeria vaccine

expressing mesothelin (CRS-207) for advanced cancers: Phase I studies of safety and immune induction. Clin. Cancer Res. *18*, 858–868.

12. Hassan, R., Alley, E., Kindler, H., Antonia, S., Jahan, T., Honarmand, S., Nair, N., Whiting, C.C., Enstrom, A., Lemmens, E., et al. (2019). Clinical Response of Live-Attenuated, Listeria monocytogenes Expressing Mesothelin (CRS-207) with Chemotherapy in Patients with Malignant Pleural Mesothelioma. Clin. Cancer Res. *25*, 5787–5798.
13. Tsujikawa, T., Crocenzi, T., Durham, J.N., Sugar, E.A., Wu, A.A., Onners, B., Nauroth, J.M., Anders, R.A., Fertig, E.J., Laheru, D.A., et al. (2020). Evaluation of Cyclophosphamide/GVAX Pancreas Followed by Listeria-Mesothelin (CRS-207) with or without Nivolumab in Patients with Pancreatic Cancer. Clin. Cancer Res. *26*, 3578–3588. https://doi.org/10.1158/1078-0432.CCR-19-3978.
14. Le, D.T., Wang-Gillam, A., Picozzi, V., Greten, T.F., Crocenzi, T., Springett, G., Morse, M., Zeh, H., Cohen, D., Fine, R.L., et al. (2015). Safety and survival with GVAX pancreas prime and Listeria monocytogenes-expressing mesothelin (CRS-207) boost vaccines for metastatic pancreatic cancer. J. Clin. Oncol. *33*, 1325–1333.
15. Corrales, L., Glickman, L.H., McWhirter, S.M., Kanne, D.B., Sivick, K.E., Katibah, G.E., Woo, S.R., Lemmens, E., Banda, T., Leong, J.J., et al. (2015). Direct Activation of STING in the Tumor Microenvironment Leads to Potent and Systemic Tumor Regression and Immunity. Cell Rep. *11*, 1018–1030.
16. Fu, J., Kanne, D.B., Leong, M., Glickman, L.H., McWhirter, S.M., Lemmens, E., Mechette, K., Leong, J.J., Lauer, P., Liu, W., et al. (2015). STING agonist formulated cancer vaccines can cure established tumors resistant to PD-1 blockade. Sci. Transl. Med. *7*, 283ra52.
17. Demaria, O., De Gassart, A., Coso, S., Gestermann, N., Di Domizio, J., Flatz, L., Gaide, O., Michielin, O., Hwu, P., Petrova, T.V., et al. (2015). STING activation of tumor endothelial cells initiates spontaneous and therapeutic antitumor immunity. Proc. Natl. Acad. Sci. USA *112*, 15408–15413.
18. Flood, B.A., Higgs, E.F., Li, S., Luke, J.J., and Gajewski, T.F. (2019). STING pathway agonism as a cancer therapeutic. Immunol. Rev. *290*, 24–38.
19. Francica, B.J., Ghasemzadeh, A., Desbien, A.L., Theodros, D., Sivick, K.E., Reiner, G.L., Hix Glickman, L., Marciscano, A.E., Sharabi, A.B., Leong, M.L., et al. (2018). TNFa and radioresistant stromal cells are essential for therapeutic efficacy of cyclic dinucleotide STING agonists in nonimmunogenic tumors. Cancer Immunol. Res. *6*, 422–433.
20. Sivick, K.E., Desbien, A.L., Glickman, L.H., Reiner, G.L., Corrales, L., Surh, N.H., Hudson, T.E., Vu, U.T., Francica, B.J., Banda, T., et al. (2018). Magnitude of Therapeutic STING Activation Determines CD8+ T Cell-Mediated Anti-tumor Immunity. Cell Rep. *25*, 3074–3085.e5.
21. Nicolai, C.J., Wolf, N., Chang, I.C., Kirn, G., Marcus, A., Ndubaku, C.O., McWhirter, S.M., and Raulet, D.H. (2020). NK cells mediate clearance of CD8+ T cell-resistant tumors in response to STING agonists. Sci. Immunol. *5*, eaaz2738.
22. Meric-Bernstam, F., Sweis, R.F., Kasper, S., Hamid, O., Bhatia, S., Dummer, R., Stradella, A., Long, G.V., Spreafico, A., Shimizu, T., et al. (2023). Combination of the STING Agonist MIW815 (ADU-S100) and PD-1 Inhibitor Spartalizumab in Advanced/Metastatic Solid Tumors or Lymphomas: An Open-Label, Multicenter, Phase Ib Study. Clin. Cancer Res. *29*, 110–121.
23. Meric-Bernstam, F., Sweis, R.F., Hodi, F.S., Messersmith, W.A., Andtbacka, R.H.I., Ingham, M., Lewis, N., Chen, X., Pelletier, M., Chen, X., et al. (2022). Phase I Dose-Escalation Trial of MIW815 (ADU-S100), an Intratumoral STING Agonist, in Patients with Advanced/Metastatic Solid Tumors or Lymphomas. Clin. Cancer Res. *28*, 677–688.
24. Brockstedt, D.G., Giedlin, M.A., Leong, M.L., Bahjat, K.S., Gao, Y., Luckett, W., Liu, W., Cook, D.N., Portnoy, D.A., and Dubensky, T.W., Jr. (2004). Listeria-based cancer vaccines that segregate immunogenicity from toxicity. Proc. Natl. Acad. Sci. USA *101*, 13832–13837.
25. Auerbuch, V., Lenz, L.L., and Portnoy, D.A. (2001). Development of a competitive index assay to evaluate the virulence of Listeria monocytogenes actA mutants during primary and secondary infection of mice. Infect. Immun. *69*, 5953–5957.
26. Burke, T.P., Engström, P., Tran, C.J., Langohr, I.M., Glasner, D.R., Espinosa, D.A., Harris, E., and Welch, M.D. (2021). Interferon receptor-deficient mice are susceptible to eschar-associated rickettsiosis. eLife *10*, e67029.
27. Burke, T.P., Engström, P., Tran, C.J., Glasner, D.R., Espinosa, D.A., Harris, E., and Welch, M.D. (2020). Interferon receptor-deficient mice are susceptible to eschar-associated rickettsiosis. Preprint at bioRxiv. https://doi.org/10.1101/2020.09.23.310409.
28. Rameshbabu, S., Labadie, B.W., Argulian, A., and Patnaik, A. (2021). Targeting innate immunity in cancer therapy. Vaccines *9*, 138.
29. Machata, S., Tchatalbachev, S., Mohamed, W., Jänsch, L., Hain, T., and Chakraborty, T. (2008). Lipoproteins of Listeria monocytogenes are critical for virulence and TLR2-mediated immune activation. J. Immunol. *181*, 2028–2035.
30. de Queiroz, N.M.G.P., Marinho, F.V., de Araujo, A.C.V.S.C., Fahel, J.S., and Oliveira, S.C. (2021). MyD88-dependent BCG immunotherapy reduces tumor and regulates tumor microenvironment in bladder cancer murine model. Sci. Rep. *11*, 15648.
31. Alspach, E., Lussier, D.M., and Schreiber, R.D. (2019). Interferon γ and Its Important Roles in Promoting and Inhibiting Spontaneous and Therapeutic Cancer Immunity. Cold Spring Harb. Perspect. Biol. *11*, a028480.
32. Sharma, N., Vacher, J., and Allison, J.P. (2019). TLR1/2 ligand enhances antitumor efficacy of CTLA-4 blockade by increasing intratumoral Treg depletion. Proc. Natl. Acad. Sci. USA *116*, 10453–10462.
33. Gulen, M.F., Koch, U., Haag, S.M., Schuler, F., Apetoh, L., Villunger, A., Radtke, F., and Ablasser, A. (2017). Signalling strength determines proapoptotic functions of STING. Nat. Commun. *8*, 427.
34. Luke, J.J., Piha-Paul, S.A., Medina, T., Verschraegen, C.F., Varterasian, M., Brennan, A.M., Riese, R.J., Sokolovska, A., Strauss, J., Hava, D.L., and Janku, F. (2023). Phase I Study of SYNB1891, an Engineered E. coli Nissle Strain Expressing STING Agonist, with and without Atezolizumab in Advanced Malignancies. Clin. Cancer Res. *29*, 2435–2444.
35. Leventhal, D.S., Sokolovska, A., Li, N., Plescia, C., Kolodziej, S.A., Gallant, C.W., Christmas, R., Gao, J.R., James, M.J., Abin-Fuentes, A., et al. (2020). Immunotherapy with engineered bacteria by targeting the STING pathway for anti-tumor immunity. Nat. Commun. *11*, 2739.
36. Bhatnagar, S., Revuri, V., Shah, M., Larson, P., Shao, Z., Yu, D., Prabha, S., Griffith, T.S., Ferguson, D., and Panyam, J. (2022). Combination of STING and TLR 7/8 Agonists as Vaccine Adjuvants for Cancer Immunotherapy. Cancers *14*, 6091.
37. Hajiabadi, S., Alidadi, S., Montakhab Farahi, Z., Ghahramani Seno, M.M., Farzin, H., and Haghparast, A. (2023). Immunotherapy with STING and TLR9 agonists promotes synergistic therapeutic efficacy with suppressed cancer-associated fibroblasts in colon carcinoma. Front. Immunol. *14*, 1258691.
38. Castro Eiro, M.D., Hioki, K., Li, L., Wilmsen, M.E.P., Kiernan, C.H., Brouwers-Haspels, I., van Meurs, M., Zhao, M., de Wit, H., Grashof, D.G.B., et al. (2024). TLR9 plus STING Agonist Adjuvant Combination Induces Potent Neopeptide T Cell Immunity and Improves Immune Checkpoint Blockade Efficacy in a Tumor Model. J. Immunol. *212*, 455–465. https://doi.org/10.4049/jimmunol.2300038.
39. Zhang, B.-D., Wu, J.J., Li, W.H., Hu, H.G., Zhao, L., He, P.Y., Zhao, Y.F., and Li, Y.M. (2022). STING and TLR7/8 agonists-based nanovaccines for synergistic antitumor immune activation. Nano Res. *15*, 6328–6339.
40. Kocabas, B.B., Almacioglu, K., Bulut, E.A., Gucluler, G., Tincer, G., Bayik, D., Gursel, M., and Gursel, I. (2020). Dual-adjuvant effect of pH-sensitive liposomes loaded with STING and TLR9 agonists regress tumor development by enhancing Th1 immune response. J. Control. Release *328*, 587–595.
41. Lorkowski, M.E., Atukorale, P.U., Bielecki, P.A., Tong, K.H., Covarrubias, G., Zhang, Y., Loutrianakis, G., Moon, T.J., Santulli, A.R., Becicka, W.M.,

and Karathanasis, E. (2021). Immunostimulatory nanoparticle incorporating two immune agonists for the treatment of pancreatic tumors. J. Control. Release *330*, 1095–1105.

42. Mai, J., Li, Z., Xia, X., Zhang, J., Li, J., Liu, H., Shen, J., Ramirez, M., Li, F., Li, Z., et al. (2021). Synergistic Activation of Antitumor Immunity by a Particulate Therapeutic Vaccine. Adv. Sci. *8*, 2100166.
43. Temizoz, B., Kuroda, E., Ohata, K., Jounai, N., Ozasa, K., Kobiyama, K., Aoshi, T., and Ishii, K.J. (2015). TLR9 and STING agonists synergistically induce innate and adaptive type-II IFN. Eur. J. Immunol. *45*, 1159–1169.
44. Temizoz, B., Hioki, K., Kobari, S., Jounai, N., Kusakabe, T., Lee, M.S.J., Coban, C., Kuroda, E., and Ishii, K.J. (2022). Anti-tumor immunity by transcriptional synergy between TLR9 and STING activation. Int. Immunol. *34*, 353–364.
45. Alvarez, M., Molina, C., De Andrea, C.E., Fernandez-Sendin, M., Villalba, M., Gonzalez-Gomariz, J., Ochoa, M.C., Teijeira, A., Glez-Vaz, J., Aranda, F., et al. (2021). Intratumoral co-injection of the poly I:C-derivative BO-112 and a STING agonist synergize to achieve local and distant anti-tumor efficacy. J. Immunother. Cancer *9*, e002953.
46. Borden, E.C. (2019). Interferons α and β in cancer: therapeutic opportunities from new insights. Nat. Rev. Drug Discov. *18*, 219–234.
47. Woo, S.-R., Fuertes, M.B., Corrales, L., Spranger, S., Furdyna, M.J., Leung, M.Y.K., Duggan, R., Wang, Y., Barber, G.N., Fitzgerald, K.A., et al. (2014). STING-Dependent Cytosolic DNA Sensing Mediates Innate Immune Recognition of Immunogenic Tumors. Immunity *41*, 830–842.
48. Sauer, J.D., Sotelo-Troha, K., von Moltke, J., Monroe, K.M., Rae, C.S., Brubaker, S.W., Hyodo, M., Hayakawa, Y., Woodward, J.J., Portnoy, D.A., and Vance, R.E. (2011). The N-ethyl-N-nitrosourea-induced Goldenticket mouse mutant reveals an essential function of sting in the in vivo interferon response to Listeria monocytogenes and cyclic dinucleotides. Infect. Immun. *79*, 688–694.
49. Marcus, A., Mao, A.J., Lensink-Vasan, M., Wang, L., Vance, R.E., and Raulet, D.H. (2018). Tumor-Derived cGAMP Triggers a STING-Mediated Interferon Response in Non-tumor Cells to Activate the NK Cell Response. Immunity *49*, 754–763.e4.
50. Borgo, G.M., Burke, T.P., Tran, C.J., Lo, N.T.N., Engström, P., and Welch, M.D. (2022). A patatin-like phospholipase mediates Rickettsia parkeri escape from host membranes. Nat. Commun. *13*, 3656.
51. Engström, P., Burke, T.P., Mitchell, G., Ingabire, N., Mark, K.G., Golovkine, G., Iavarone, A.T., Rape, M., Cox, J.S., and Welch, M.D. (2019). Evasion of autophagy mediated by Rickettsia surface protein OmpB is critical for virulence. Nat. Microbiol. *4*, 2538–2551.
52. Engström, P., Burke, T.P., Tran, C.J., Iavarone, A.T., and Welch, M.D. (2021). Lysine methylation shields an intracellular pathogen from ubiquitylation and autophagy. Sci. Adv. *7*, eabg2517.
53. Ahyong, V., Berdan, C.A., Burke, T.P., Nomura, D.K., and Welch, M.D. (2019). A Metabolic Dependency for Host Isoprenoids in the Obligate Intracellular Pathogen Rickettsia parkeri Underlies a Sensitivity to the Statin Class of Host-Targeted Therapeutics. mSphere *4*, e00536-19.

STAR★METHODS

KEY RESOURCES TABLE

REAGENT or RESOURCE	SOURCE	IDENTIFIER
Antibodies		
anti-CD8b.2	Leinco	C2832; RRID:AB_2737471
IgG control	Jackson Labs	012-000-003; RRID:AB_2337136
Bacterial and virus strains		
Listeria monocytogenes ΔactA ΔinlB	Dan Portnoy (UC Berkeley)	
Rickettsia parkeri sca2:Tn	Matt Welch (UC Berkeley)	
Rickettsia parkeri (WT)	Matt Welch (UC Berkeley)	
Burkholderia thailandensis ΔbimA ΔmotA2	Jeff Miller (UCLA)	
Listeria monocytogenes ΔactA ΔinlB	Dan Portnoy (UC Berkeley)	
Rickettsia parkeri sca2:Tn	Matt Welch (UC Berkeley)	
Rickettsia parkeri (WT)	Matt Welch (UC Berkeley)	
Burkholderia thailandensis ΔbimA ΔmotA2	Jeff Miller (UCLA)	
Listeria monocytogenes delta hly	Dr. Dan Portnoy (UC Berkeley)	
Chemicals, peptides, and recombinant proteins		
PAM3CSK4	Invivogen	vac-pms
S100 (MIW815)	Chemietek	CT-ADUS100
Deposited data		
Dryad		https://doi.org/10.5061/dryad.n2z34tn5z
Experimental models: Cell lines		
B16-F10 cells	ATCC	CRL-6475; **RRID:CVCL_0159**
RMA cells	Dr. David Raulet, (obtained from M. Bevan, who received it from K. Karre, Karolinska Institute, Stockholm, Sweden)	
B16-BL6 cells	Dr. David Raulet	
B16-BL6 Cgas−/− cells	Dr. David Raulet	
Experimental models: Organisms/strains		
WT mouse - C57bl6/J	Jackson Labs	000664; **RRID:IMSR_JAX:000664**
Ifnar−/− mice - Jackson	Jackson labs	028288 **RRID:IMSR_JAX:028288**
Rag2−/− mouse	Jackson labs	008449 **RRID:IMSR_JAX:008449**
Ifngr −/− mouse	Jackson labs	003288; **RRID:IMSR_JAX:003288**
Cgas−/− mouse	Dr. David Raulet (UC Berkeley)	
Sting -gt/gt mouse	Dr. Russell Vance (UC Berkeley)	
Myd88/TRIF−/− mice	Dr. Greg Barton (UC Berkeley)	
Oligonucleotides		
cGAS Forward	ACTGGGAATCCAGCTTTTCACT	
cGAS Reverse	TGGGGTCAGAGGAAATCAGC	
Sting Forward	GATCCGAATGTTCAATCAGC	
Sting reverse	CGATTCTTGATGCCAGCAC	
Ifnar Forward	CAACATACTACAACGACCAAGTGTG	
Ifnar Reverse	AACAAACCCCCAAACCCCAG	
Ifnar mutant	ATCTGGACGAAGAGCATCAGG	
cGAS Forward	ACTGGGAATCCAGCTTTTCACT	
cGAS Reverse	TGGGGTCAGAGGAAATCAGC	
Sting Forward	GATCCGAATGTTCAATCAGC	

(*Continued on next page*)

Continued

REAGENT or RESOURCE	SOURCE	IDENTIFIER
Sting reverse	CGATTCTTGATGCCAGCAC	
Ifnar Forward	CAACATACTACAACGACCAAGTGTG	
Ifnar Reverse	AACAAACCCCCAAACCCCAG	
Ifnar mutant	ATCTGGACGAAGAGCATCAGG	
Software and algorithms		
Graphpad Prism		

EXPERIMENTAL MODEL AND STUDY PARTICIPANT DETAILS

Animal maintenance

Animal research using mice was conducted under a protocol approved by the UC Irvine and the UC Berkeley Institutional Animal Care and Use Committee (IACUC) in compliance with the Animal Welfare Act and other federal statutes relating to animals and experiments using animals (Burke lab animal use protocol AUP-22-005, Welch lab animal use protocol AUP-2016-02-8426). The UC Irvine and Berkeley IACUCs are fully accredited by the Association for the Assessment and Accreditation of Laboratory Animal Care International and adheres to the principles of the Guide for the Care and use of Laboratory Animals. Infections were performed in a biosafety level 2 facility and all animals were maintained at the UC Irvine or Berkeley campus. All mice were healthy at the time of tumor delivery and were housed in microisolator cages and provided chow and water. No mice were administered antibiotics or maintained on water with antibiotics. Mice were euthanized if a tumor measured >15 mm in any direction. Mice were between 8 and 24 weeks old at the time of tumor delivery and all mice were of the C57BL/6J background. Mice were selected for experiments based on their availability and littermates within the same cage were assigned to different groups. Both male and female mice were used in all groups. Initial sample sizes were based on availability of mice, which were approximately 5 mice per group and a minimum of 3 mice per group. Therapeutic treatments were assigned to mice such that each group was divided into as many cages as possible and with a similar number of male/female mice between each cohort (mixed cohorts). Power analyses were conducted after initial experiments to determine subsequent group sizes.

Mouse genotyping

Sting$^{gt/gt}$ and *Cgas*$^{-/-}$ mice were generated as previously described.[48,49] *Ifnar*$^{-/-}$, *Ifngr*$^{-/-}$, and *Rag2*$^{-/-}$ mice were obtained from Jackson Labs. C57BL/6J WT mice were originally obtained from Jackson Laboratories. For genotyping, ear clips were boiled for 15 min in 60 μL of 25 mM NaOH, quenched with 10 μL tris-HCl pH 5.5, and 2 μL of lysate was used for PCR using SapphireAMP (Takara, RR350) and primers specific for each gene. Mice were genotyped using these primers: *Cgas* F: ACTGGGAA TCCAGCTTTTCACT; *Cgas* R: TGGGGTCAGAGGAAATCAGC; *Sting* F: GATCCGAATGTTCAATCAGC; *Sting* R: CGATTCTTGATG CCAGCAC; *Ifnar* forward (F): CAACATACTACAACGACCAAGTGTG; *Ifnar* WT reverse (R): AACAAACCCCCAAACCCCAG; and *Ifnar* mutant R: ATCTGGACGAAGAGCATCAGG.

Bacterial strains

Rp strain Portsmouth was originally obtained from Christopher Paddock (Centers for Disease Control and Prevention). *Lm* and *Bt* were prepared by inoculating 2 mL liquid brain heart infusion (BHI) media into 14 mL conical tubes and growing the bacteria for 20 h shaking at a slant at 37°C. Bacteria were then diluted 1:40 into 2 mL fresh BHI and grown for 2 h. OD_{600} for each sample was measured, bacteria were centrifuged and washed once with sterile room temperature PBS, and resuspended in PBS to a concentration of 10^7 or 10^6/50 μL. *Lm* and *Bt* were kept at room temperature prior to injection and delivered intratumorally using 30.5 gauge needles. Bacteria were serially diluted and plated on LB plates to verify the inoculum. All *Lm* strains were a generous gift from Dr. Dan Portnoy (UC Berkeley). All *Bt* strains were a generous gift from Dr. Jeff Miller (UCLA). All *Rp* strains were a generous gift from Dr. Matt Welch. *Rp* strains were authenticated by whole genome sequencing and are available in the NCBI Trace and Short-Read Archive; Sequence Read Archive (SRA), accession number SRX4401164.

Preparation of bacteria

Bacteria were amplified by infecting confluent T175 flasks of female African green monkey kidney epithelial Vero cells authenticated by mass spectrometry. WT and *sca2* mutant *Rp* stocks were purified and quantified as described.[50–53] For mouse infections, *Rp* was prepared by diluting 30%-prep bacteria into sterile PBS on ice, centrifuging the bacteria at 12,000 x G for 1 min (Eppendorf 5430 centrifuge), and resuspended in cold sterile PBS to the desired concentration (either 10^7 PFU/50 μL or 10^6 PFU/50 μL). Bacterial suspensions were kept on ice during injections. Mice were scruffed and 50 μL of bacterial suspensions were injected using 30.5-gauge needles into palpable tumors. Body temperatures were monitored using a rodent rectal thermometer (BrainTree Scientific, RET-3). $CD8^+$ T cells were depleted by injecting mice IP with 160 μg of α-CD8b.2 (Leinco C2832) on days −2 and −1 prior to infection (320 μg

total per mouse). For depletion control experiments, 100 μg of control IgG antibody (Jackson, 012-000-003) was delivered IP. After infection, all mice in this study were monitored daily for clinical signs of disease, such as hunched posture, lethargy, or scruffed fur.

Deriving bone marrow macrophages

To obtain bone marrow, male or female mice were euthanized, and femurs, tibias, and fibulas were excised. Connective tissue was removed, and the bones were sterilized with 70% ethanol. Bones were washed with BMDM media (20% FBS, 1% sodium pyruvate, 0.1% β-mercaptoethanol, 10% conditioned supernatant from 3T3 fibroblasts, in Gibco DMEM containing glucose and 100 U/ml penicillin and 100 μg/ml streptomycin) and ground using a mortar and pestle. Bone homogenate was passed through a 70 μm nylon Corning Falcon cell strainer (Thermo Fisher Scientific, 08-771-2) to remove particulates. Filtrates were centrifuged in an Eppendorf 5810R at 1,200 RPM (290 x G) for 8 min, supernatant was aspirated, and the remaining pellet was resuspended in BMDM media. Cells were then plated in non-TC-treated 15 cm petri dishes (at a ratio of 10 dishes per 2 femurs/tibias) in 30 mL BMDM media and incubated at 37°C. An additional 30 mL was added 3 days later. At 7 days the media was aspirated, and cells were incubated at 4°C with 15 mL cold PBS (Gibco, 10010-023) for 10 min. BMDMs were then scraped from the plate, collected in a 50 mL conical tube, and centrifuged at 1,200 RPM (290 x G) for 5 min. The PBS was then aspirated, and cells were resuspended in BMDM media with 30% FBS and 10% DMSO at 10^7 cells/ml. 1 mL aliquots were stored in liquid nitrogen.

METHOD DETAILS

Tumor xenografts and intratumoral deliveries

B16-F10 cells were obtained and authenticated from ATCC. B16-F10 and B16-B6 were grown *in vitro* in DMEM (Gibco 11965-092) supplemented with 10% fetal bovine serum (FBS, Corning 35-010-CV). *Cgas*−/− B16-BL6 cells[49] and RMA cells were a generous gift from Dr. David Raulet (UC Berkeley). RMA cells were grown in suspension in RPMI supplemented with 10% FBS. All cell lines were periodically tested for the presence of *Mycoplasma* with the Abcam *Mycoplasma* testing kit (AB289834) and were determined to be negative. Prior to injection, cells were trypsinized, counted, washed with sterile PBS, and resuspended at 1-3x10^6 cells/100 μL. Mice were shaved on their right hind flank and injected subcutaneously with tumor cells in 100 μL volumes. Tumor size was monitored by measuring the length, width, and height of each tumor using calipers. Reported tumor volumes were calculated as ellipsoids, where V = (length × width × height)*3.1415/6, as described previously.[21] Tumors were injected when they had reached the approximate dimensions of 6 × 6 × 2.5 mm, no tumors were injected when the tumor volume was below 65 mm^3 as calculated by length x width x height.

Vaccigrade PAM3CSK4 was from Invivogen (catalog vac-pms). S100 (MIW815) was from Chemietek or was originally generated by Aduro Biotech and provided as a gift from Dr. David Raulet (UC Berkeley). These molecules were resuspended in sterile PBS pH 7.4 and stored at −20° C prior to injection in 100 μL volumes. For combination therapies, drugs were mixed immediately prior to injection.

Infections *in vitro*

To plate cells for infection, aliquots of BMDMs were thawed on ice, diluted into 9 mL of DMEM, centrifuged in an Eppendorf 5810R at 1,200 RPM (290 x G) for 5 min, and the pellet was resuspended in 10 mL BMDM media without antibiotics. The number of cells was counted using Trypan blue (Sigma, T8154) and a hemocytometer (Bright-Line), and 5 x 10^5 cells were plated into 24-well plates. For infections with *Rp*, approximately 16 h later, 30% prep *Rp* were thawed on ice and diluted into fresh BMDM media to the desired concentration for an MOI of 1. Media was then aspirated from the BMDMs, replaced with 500 μL media containing *Rp,* and plates were spun at 300 G for 5 min in an Eppendorf 5810R. Infected cells were then incubated in a humidified CEDCO 1600 incubator set to 33°C and 5% CO_2 for the duration of the experiment. For infections with *Lm* and *Bt,* cultures were grown in 2 mL sterile-filtered BHI shaking at 37° to stationary phase (∼16 h). Cultures were centrifuged at 20,000 x G (Eppendorf 5430), the pellet was resuspended in sterile PBS and diluted to 5 × 10^7 CFU/ml, and 10 μL were added to each well. Bacteria were plated onto Luria Broth agarose plates to determine the titer, which was determined to be ∼5 x 10^5 bacteria/10 μL, for an MOI of 1 (based on the ratio of bacteria in culture to number of BMDMs). Infected cells were incubated in a humidified 37° incubator with 5% CO_2. For *Lm*, a final concentration of 50 μg/mL of gentamicin (Gibco 15710-064) was added to each well at 1 hpi. For *Bt*, 500 μg/mL final concentration of gentamicin was added at 1 hpi. At 30 mpi, 2, 5, and 8 hpi, the supernatant was aspirated from infected cells, and cells were washed twice with sterile Milli-Q water. Infected BMDMs were then lysed with 1 mL sterile water by repeated pipetting and scraping of the well. Lysates were then serially diluted and plated on LB agar plates, incubated at 37° overnight, and CFU were counted at ∼20 h later.

In vitro assays

For the IFN-I bioassay, 5 x 10^4 3T3 cells containing an interferon-sensitive response element (ISRE) fused to luciferase were plated per well into 96-well white-bottom plates (Greneir 655083) in DMEM containing 10% FBS, 100 U/ml penicillin and 100 μg/mL streptomycin. Media was replaced 24 h later and confluent cells were treated with 2 μL of supernatant harvested from BMDM experiments. Media was removed 4 h later and cells were lysed with 40 μL TNT lysis buffer (20 mM Tris, pH 8, 200 mM NaCl, 1% triton-100). Lysates were then injected with 40 μL firefly luciferin substrate and luminescence was measured using the luminometer function of the ClarioStar-Plus plate reader.

QUANTIFICATION AND STATISTICAL ANALYSIS

For tumor growth, comparisons were made using two-way ANOVAs without an interaction term and not assuming sphericity (Geisser-Greenhouse correction). Log rank (Mantel-Cox) tests were used for survival. *In vitro* data used a one-way ANOVA with Tukey's multiple comparisons test. Data are determined to be statistically significant when $p < 0.05$. For tumor growth curves, data are the means and error bars represent the standard error of the mean (SEM). Asterisks denote statistical significance as: *, $p < 0.05$; **, $p < 0.01$; ***, $p < 0.001$; ****, $p < 0.0001$. On days when tumors were not measured, the growth in tumor volume was calculated by taking the difference between tumor volumes at adjacent time points. In compiled tumor volume data, if a mouse was euthanized due to a tumor measuring >15 mm in any direction, the final tumor volume for that mouse was duplicated until either day 20 or until the last mouse in that group was euthanized. Statistical analyses were performed using GraphPad PRISM V9. Statistical parameters and significance are also reported in the figure legends.